ACS MATERIALS LETTERS

www.acsmaterialsletters.org

LETTER

Thermal Activation of a Copper-Loaded Covalent Organic Framework for Near-Ambient Temperature Hydrogen Storage and Delivery

Wade A. Braunecker,* Sarah Shulda, Madison B. Martinez, Katherine E. Hurst, Joshua T. Koubek, Sarah Zaccarine, Rachel E. Mow, Svitlana Pylypenko, Alan Sellinger, Thomas Gennett, and Justin C. Johnson*

Cite This: *ACS Materials Lett.* 2020, 2, 227−232

Read Online

ACCESS | Metrics & More | Article Recommendations | Supporting Information

ABSTRACT: Copper(II) formate is efficiently incorporated into the pores of a 2D imine-based covalent organic framework (COF) via coordination with the phenol and imine groups. The coordinated metal ion is then reduced to Cu(I) with a thermal treatment that evolves CO_2. After loading with hydrogen gas, the majority of H_2 desorbs from the coordinatively saturated Cu(II) COF at temperatures < −100 °C. However, the activated Cu(I) COF retains adsorbed H_2 above room temperature. Adsorption/desorption of H_2 was highly reversible. Diffuse reflectance infrared Fourier transform spectroscopy (DRIFTS) strongly supports a molecular hydrogen interaction with Cu(I). A Kissinger analysis of variable ramp rate desorption experiments estimates the enthalpy of H_2 desorption from Cu(I) at 15 kJ mol^{-1}. The results represent an advance toward practical H_2 storage and delivery in a lightweight, stable, and highly versatile material.

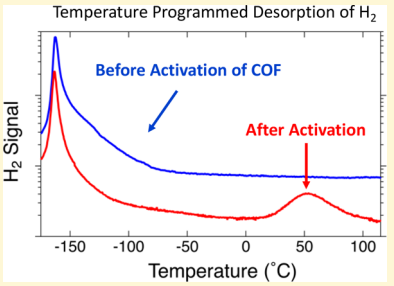

The structural diversity of covalent organic frameworks (COFs) has made these high surface area materials attractive across a broad spectrum of research fields in the last decade.[1−3] Countless permutations of COFs have appeared in recent years with targeted applications in the fields of energy storage,[4,5] optoelectronics,[6,7] catalysis,[8−10] environmental remediation,[11,12] etc. While they have also been well-studied as gas sorbent and storage materials, particularly for CO_2,[13−15] the physisorption of H_2 to solid surfaces of most framework materials is quite weak. Adsorption enthalpies are typically in the range of 5−9 kJ mol^{-1},[16] which necessitates cryogenic temperatures for long-term H_2 storage in these materials. Enthalpies larger than this are quite rare and are usually found in sorbent materials that impart some unique metal−hydrogen interaction.[17,18] Adsorption enthalpies between 15−25 kJ mol^{-1} are generally considered near optimal for ambient temperature storage and delivery.[19] Successful strategies that could be broadly applied to a large class of materials for enhancing and tuning H_2 binding enthalpies in solid state sorbent materials could have profound implications on the overall viability of large-scale H_2 storage and distribution.

Recent computational analyses using quantum mechanical methods have suggested that metal-loaded COFs should in principle be capable of dramatically enhancing H_2 binding enthalpy so as to meet or exceed most volumetric capacity targets for H_2 storage set by the Department of Energy.[20] In practice, however, attaining coordinately unsaturated metal-sites in these materials is not trivial; the small framework pores can become clogged/blocked during post-synthetic metalation[20] or "activation" of binding sites by removing solvent or solvating ligand will often trigger partial pore collapse in framework materials.[21]

One intriguing example of a successful strategy for activating a framework-based material to achieve a coordinatively unsaturated metal center was recently developed for a metal−organic framework (MOF) loaded with copper and zinc.[22] The so-called Cu(I)-MFU-4l MOF employs charged triazolate ligands which bind Cu in tridentate fashion, analogous to scorpionate type complexes.[23] Charge-balance of the Cu(II) species is achieved with one formate counterion. A thermal treatment of this MOF at 180 °C under vacuum

Received: September 27, 2019
Accepted: January 31, 2020
Published: January 31, 2020

https://dx.doi.org/10.1021/acsmaterialslett.9b00413
ACS Materials Lett. 2020, 2, 227−232

Scheme 1. Synthesis of COF, Loading with Cu^{II} Formate, and Thermal Treatment to Generate Open Cu^{I} Binding Sites

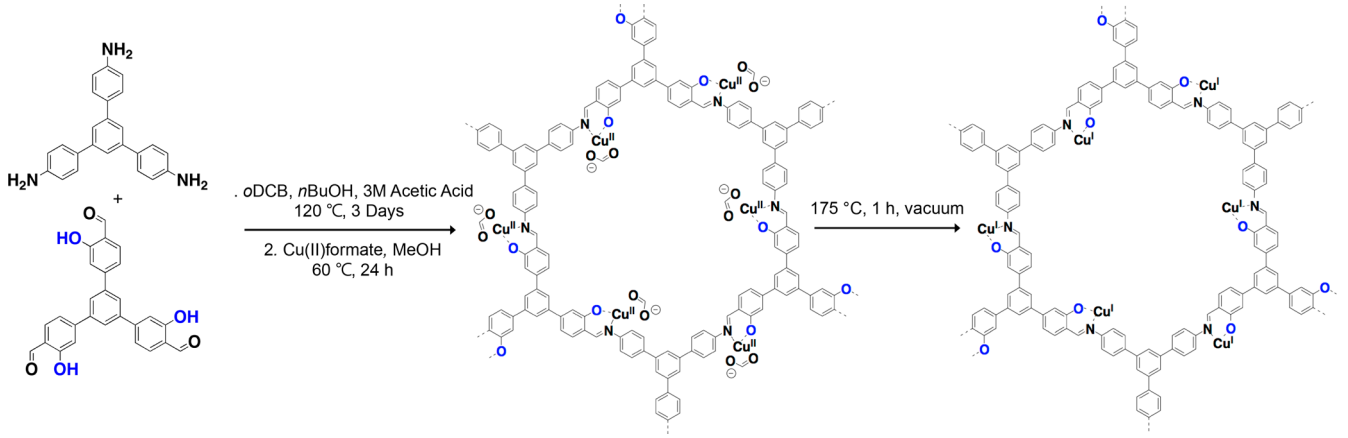

results in copper reduction to Cu(I) by the formate ion, which subsequently evolves from the material under vacuum as CO_2, leaving a coordinatively unsaturated tridentate Cu(I) species. The 32 kJ mol^{-1} binding enthalpy of this activated Cu(I) MOF for H_2 is remarkably strong for a small nonpolar gas molecule.[22]

Here, we employ an imine-based 2D COF (OH−COF, Scheme 1) capable of intramolecular hydrogen bonding between the phenolic hydrogen and the imine within the framework. This particular COF was recently developed by our group as part of a larger effort to improve crystallinity and long-range order in 2D COF materials,[24] but the general strategy had already been routinely employed as a means to suppress torsion between neighboring moieties in the framework, thereby "locking" the 2D sheets into a planar conformation, enhancing interlayer π-stacking interactions, and effectively improving long-range order and porosity in the material.[25−27] The phenol-imine binding site (a.k.a., Schiff base) has also been employed to bind and efficiently load COFs with metals for catalysis applications.[28] Here, we load our COF with Cu(II) formate and attempt to generate an open binding site for H_2 adsorption with a thermal treatment strategy. The strategy is similar to that recently employed for the Cu(I)-MFU-4l MOF, where open metal sites were generated in the rather unique so-called Kuratowski-type units that are not easily chemically modified.[22] However, the phenol-imine moieties reported here are routinely employed throughout numerous examples of 2D and 3D literature COFs;[29] a strategy to generate coordinatively unsaturated metals at these sites could thus be transferable across a wide range of chemically tunable materials for gas storage and catalysis.

Schiff base transition metal complexes[30,31] are commonly prepared by stirring a metal complex (e.g., Cu(II) acetate) with a ligand in refluxing alcohol. Here, we used a similar procedure by mixing a two-molar excess of Cu(II) formate per available COF docking site and stirring at 60 °C in methanol overnight. The excess Cu was removed by soaking and stirring the COF over r.t. methanol for an additional 24 h, changing the solvent three times over that period. An analysis with inductively coupled plasma-atomic emission spectrometry (ICP-AES) estimated the Cu content of the COF after drying under vacuum at ∼13% by weight, corresponding to ∼70% of theoretical phenoxy-imine sites, and comparable to the 16 to 20 wt. % achieved for similar COFs with Cu(II) acetate.[28]

However, more detailed analysis of copper distribution conducted with energy-dispersive X-ray spectroscopy (EDS) in a scanning transmission electron microscope (STEM) suggested that individual COF particles showed a relatively wide range of Cu loading, and that the morphology of the COF material varied dramatically across different particles, some appearing quite porous and sponge-like (Figure 1a and b), others appearing much more dense (Figure 1c).

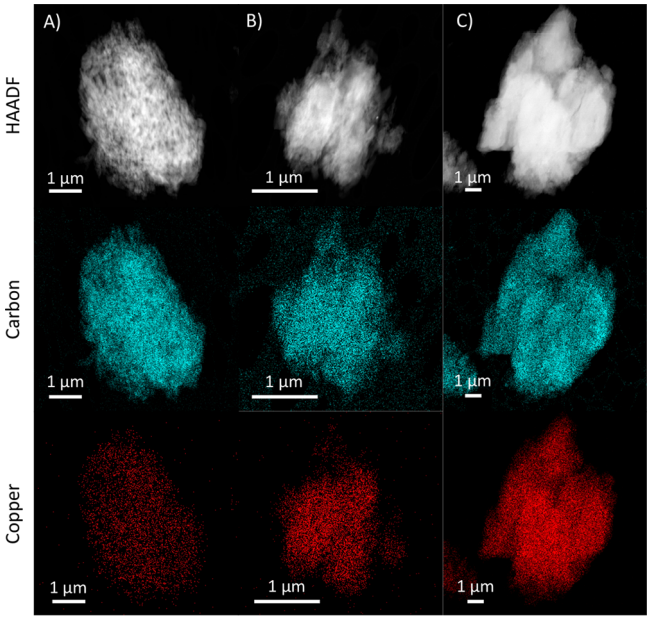

Figure 1. HAADF/STEM images and corresponding EDS maps of C (teal) and Cu (red) of three Cu-loaded COF particles, all from the same batch, but with apparent differences in morphology/porosity and Cu concentration. Some COFs displayed more porous and sponge-like morphology (A and B), while others were more dense (C).

Figure 1 illustrates our EDS elemental mapping using high-angle annular dark-field (HAADF) and scanning transmission electron microscopy (STEM) imaging. While the overall Cu content measured with this technique was 12 wt. %, consistent with the ICP analysis suggesting 13 wt. %, a "box" analysis of the EDS data (see Supporting Information for representative example) suggested that more porous particles (e.g., Figure 1a) contained only 3 wt. % Cu, more dense particles (Figure 1c)

https://dx.doi.org/10.1021/acsmaterialslett.9b00413
ACS Materials Lett. 2020, 2, 227−232

contained as much as 20 wt. % Cu, and still others (Figures 1b and S1) contained higher relative amounts of Cu at the center of the particle. These results may suggest that the less dense regions are more amorphous/disordered, and that the Cu binding sites are somehow less accessible in those regions.

A 1 g batch of the OH−COF was prepared, purified, and residual solvent was removed by pumping on the material at 100 mTorr while heating at 120 °C for 2 days. Thermogravimetric analysis (TGA) of this material suggests no significant mass loss of the material due to degradation of the framework below ∼300 °C (Figure S2). Brunauer−Emmett−Teller (BET) analysis of this 1 g batch revealed a surface area ∼1070 m^2 g^{-1}, slightly lower than the 1410 m^2/g our group previously attained on a smaller scale.[24] Being conscious of the potential for thermal activation of the Cu-loaded COF and subsequent oxidative instability, we dried the Cu(II)-COF at 40 °C for 2 days under vacuum. Mass loss occurred in this sample from the outset of the TGA analysis (Figure S2), consistent with our previous experience that more significant heat is generally required to fully remove solvents and moisture from framework materials, even under vacuum. A significant rate acceleration in mass loss was observed near 130 °C.

Using temperature-programmed desorption (TPD) coupled with a mass spectrometer, upon heating the sample at a ramp rate of 5 °C/min, we observed desorption of residual water at temperatures above 50 °C. At approximately 160 °C, a large spike in CO_2 evolution occurs (Figure 2), consistent with the

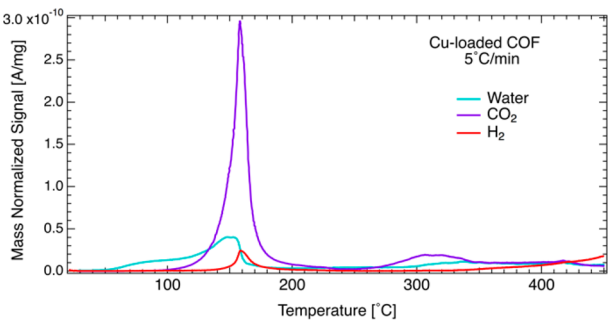

Figure 2. Temperature-programmed desorption (TPD) coupled with mass spectrometry demonstrates a spike in CO_2 evolution from the Cu(II) formate-loaded COF upon thermal treatment.

temperature at which Cu(II) formate loaded MFU-4*l* MOF is activated to Cu(I). CO_2 evolution is accompanied with a small amount of H_2 evolution, presumably a byproduct of the formate reduction. All subsequent thermal treatments of Cu-COFs were held at 175 °C under high vacuum for 1 h.

BET analysis of the Cu(II)-loaded COF indicates the integrity of the framework remains largely intact, as the material has a surface area near 860 m^2 g^{-1}, the decrease due largely to the added mass of the Cu. PXRD analysis of the parent COF and the Cu(II)-COF reveals all the original diffraction peaks are retained after Cu loading, though the overall crystallinity of the Cu(II)-COF appears lower. The pore size distribution suggests the pore width shrinks from 1.6 to 1.4 nm upon Cu loading. These results are all generally consistent with recent literature observations for the loading of Cu(II) acetate into a structurally similar COF.[28] Exactly one new peak appears in the Cu(II)-COF at ∼13 deg 2θ. Intuitively, the peak must be associated with the presence of Cu. We exclude the possibility it is residual unbound Cu(II) formate from recent literature,[32] but its origin is difficult to definitively assign.

X-ray absorption spectroscopy is a powerful technique for probing local structures without any requirements for long-range order in the material. Furthermore, the oxidation state of a metal can be obtained from the X-ray absorption near-edge structure (XANES), while information regarding that metal's coordination sphere can be extracted from the extended X-ray absorption fine structure (EXAFS).[33] As shown in the blue XANES spectrum at the top of Figure 3 corresponding to the

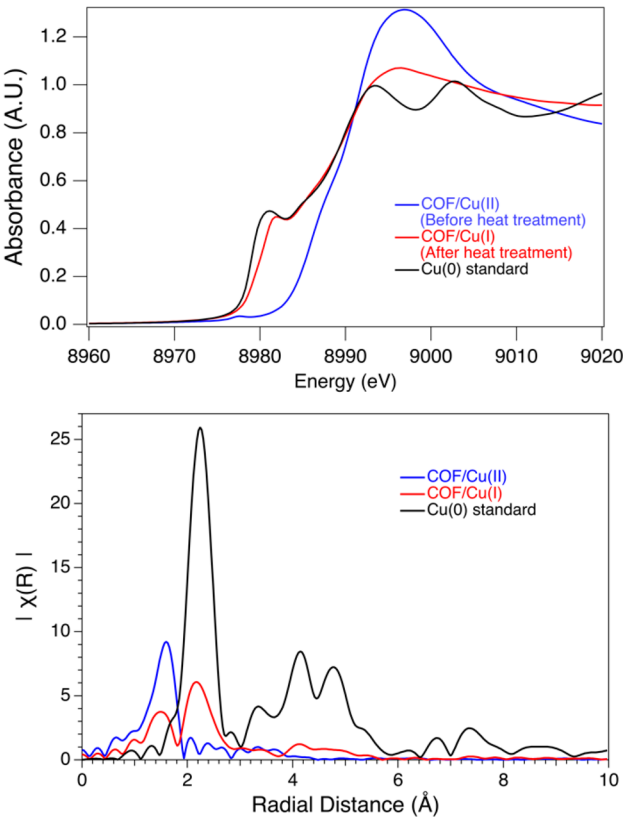

Figure 3. (Top) X-ray absorption near-edge structure (XANES) of Cu-loaded COF, before and after thermal treatment, and a copper metal reference, demonstrating definitively the reduction to the Cu(I) oxidation state. (Bottom) Extended X-ray absorption fine structure (EXAFS) of the Cu-loaded COF in its two oxidation states plotted alongside that of Cu(0) metal.

Cu(II)-COF, a weak pre-edge feature at 8977.6 eV and a shoulder at 8987 eV are observed (assigned as the 1s to 3d electron transitions and 1s to 4p or 4s transitions, respectively), as expected for Cu(II) species.[33−35] The formation of Cu(I) following the thermal treatment that evolves CO_2 is confirmed by XANES with the disappearance of the pre-edge energy and shoulder and the appearance of a peak at 8981.8 eV (1s to 4p transitions), which is fully consistent with prior assignments of Cu(I) features.[33−36] The shape of the white line peak, 8996 eV, provides evidence that Cu(II) was not reduced to Cu(0). The edge position defined by the inflection point of the 1s to 4p transitions (determined from the first maximum in the derivative of the XANES spectra), further supports Cu(I) formation. The edge is at 8986 eV for the Cu loaded COF, 8981 eV for the Cu loaded COF after heat treatment, and 8979 eV for the Cu foil, consistent with

https://dx.doi.org/10.1021/acsmaterialslett.9b00413
ACS Materials Lett. 2020, 2, 227−232

literature values for Cu(II), Cu(I), and Cu(0), respectively.[34,35]

The decrease in the feature at ~1.5 Å in the EXAFS spectrum (Figure 3, bottom) following thermal treatment of the Cu-COF (compare blue and red traces) is consistent with a reduction in the coordination sphere of Cu that would be associated with the loss of the formate anion and Cu−O bonds.[37]

Interestingly, a new feature at ~2.2 Å develops following thermal treatment of the Cu-COF. This is consistent with the major feature observed in a Cu(0) metal sample (black trace) and would thus be consistent with the formation of some new Cu−Cu interaction, plausibly the result of coordinatively unsaturated Cu(I) species being in close proximity above and below each other in different 2D COF "planes". Fitting the Fourier transform confirms that the first peak does correspond to oxygen or nitrogen in the first coordination shell of copper, and the decrease in intensity is due to a loss in Cu−O bonding (Figure S4).

H_2 desorption from these framework materials was monitored with TPD/mass spectrometry. The Cu(II)-COF was dosed with a slight over pressure of H_2 at r.t. and then quenched in a cryogenic bath. H_2 desorption was initially monitored at a ramp rate of 5 °C/min^{-1}. As can be seen it the top of Figure 4, H_2 desorption peaks near −160 °C. For the

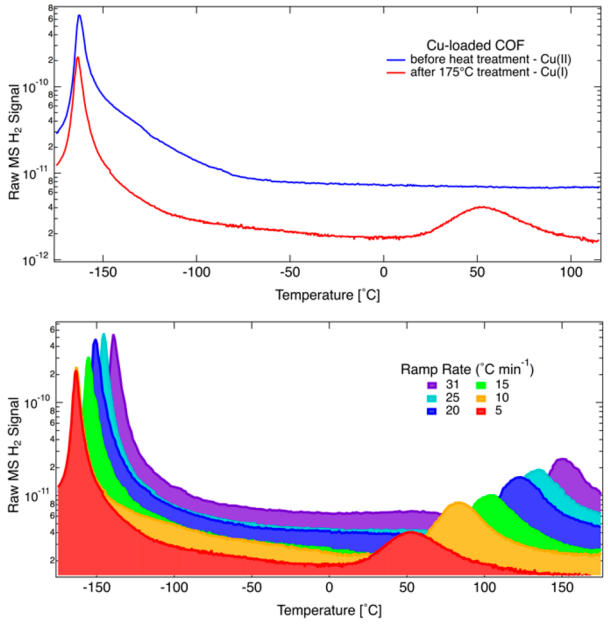

Figure 4. (Top) TPD analysis of H_2 desorption from Cu-loaded COF, before and after 175 °C thermal treatment. (Bottom) Variable temperature ramp rate data illustrating H_2 desorption used in Kissinger analysis.

activated Cu(I)-COF, H_2 desorption also peaks near −160 °C; however, a second H_2 desorption peak is observed >200 °C warmer near 50 °C. The results suggest a remarkable enhancement in H_2 binding enthalpy at specific sites in the material. Interestingly, the result is only observed when the material is dosed with H_2 above 0 °C; if dosed at cryogenic temperatures, the initial desorption of H_2 due to physisorption is observed, but the second higher enthalpy peak is not (Figure S8), suggesting a thermal activation barrier is present for H_2 adsorption to the activated metal.

In the bottom half of Figure 4, H_2 desorption from the thermally activated Cu(I)-COF is plotted as a function of six different heating rates (β). For these ramp rates, the peak temperature (T_M) for H_2 desorption varies between 50 and 150 °C. Analysis of the data according to the well-established Kissinger method, a universal approach for analyzing thermally activated transformations,[38] allows us to estimate the activation energy of H_2 desorption from a linear fit of a plot of ln (β/T_M^2) versus $1/T_M$ (Figure S7). The data suggests the activation energy for H_2 desorption from this Cu(I)-COF is ~15 kJ mol^{-1}, which is generally considered in an optimal range for ambient temperature H_2 storage and delivery. Similar analysis of the lower enthalpy binding sites in this material (bottom of Figure S7) suggest an activation energy of 4.1 kJ mol^{-1}, consistent with low values typically reported for H_2 physisorption in frameworks.[16]

Diffuse reflectance infrared Fourier transform spectroscopy (DRIFTS) results strongly support a molecular H_2 interaction with Cu(I), as opposed to the formation of a hydride complex. Following the thermal treatment under vacuum to convert Cu(II) to Cu(I), a strong but broad peak appears at approximately 3000 cm^{-1} when the COF is dosed with 1030 Torr H_2, which is attributed to the H−H stretching vibration for molecular hydrogen adsorbed to Cu(I). The peak is shifted to approximately 2200 cm^{-1} when dosed with 1030 Torr D_2 (as expected based on the difference in molecular masses of H_2 and D_2). This result aligns well with previous work reporting H_2 adsorption in Cu-modified zeolites, for which a set of low frequency bands between 3300 and 2630 cm^{-1} were connected with H_2 adsorption by Cu(I).[39] While the H−H stretching vibration for molecular H_2 adsorbed to metals can vary tremendously across different transition metal complexes (between 3200 cm^{-1} to as low as 2080 cm^{-1} for 20+ recently reviewed r.t. stable complexes), the vibrational mode of metal hydrides are observed, on average, at even lower frequencies, between 1700−2300 cm^{-1}.[40] Our DRIFTS results are thus more consistent with a molecular hydrogen-type interaction.

Pressure−composition−temperature (PCT) measurements were performed between 2 and 85 bar of H_2 at 77 K to quantify hydrogen adsorption in the material (see Figure S10 for a summary of the results). At 35 bar, 2.1 wt.% of H_2 is adsorbed in this material, fully consistent with "Chahine's rule" of ~1 wt. % per 500 m^2/g of surface area for a porous organic material.[41,42] By integrating the TPD data in Figure S8 (dosed at 50 °C and 1.5 bar of H_2), we can estimate that the H_2 capacity bound at the Cu site represents 20% of the total adsorbed H_2 capacity in the material. Furthermore, after 35 desorption cycles, no detectable loss in H_2 capacity is observed (Figure S9).

The summation of our results, coupled with the broad use of the intramolecular hydrogen bonding motif between phenolic hydrogens and imine linkages throughout numerous examples of literature COFs, suggest a whole host of potential new candidate materials lay waiting to be discovered, tuned, and optimized for gas storage/separation applications. We are actively investigating the broad applicability of this strategy with other metals and modified analogues of this COF in an attempt to establish a new class of activated gas sorbent materials with tunable desorption properties.

https://dx.doi.org/10.1021/acsmaterialslett.9b00413
ACS Materials Lett. 2020, 2, 227−232

■ ASSOCIATED CONTENT

Supporting Information

The Supporting Information is available free of charge at https://pubs.acs.org/doi/10.1021/acsmaterialslett.9b00413.

EDS mapping, TGA, X-ray absorption, DRIFTS, BET, PCT, and TPD analysis (PDF)

■ AUTHOR INFORMATION

Corresponding Authors

Wade A. Braunecker − *National Renewable Energy Laboratory, Golden, Colorado 80401, United States; Department of Chemistry, Colorado School of Mines, Golden, Colorado 80401, United States;* orcid.org/0000-0003-0773-9580; Email: Wade.Braunecker@nrel.gov

Justin C. Johnson − *National Renewable Energy Laboratory, Golden, Colorado 80401, United States; Department of Chemistry, Colorado School of Mines, Golden, Colorado 80401, United States;* orcid.org/0000-0002-8874-6637; Email: Justin.Johnson@nrel.gov

Authors

Sarah Shulda − *National Renewable Energy Laboratory, Golden, Colorado 80401, United States*

Madison B. Martinez − *National Renewable Energy Laboratory, Golden, Colorado 80401, United States; Department of Chemistry, Colorado School of Mines, Golden, Colorado 80401, United States*

Katherine E. Hurst − *National Renewable Energy Laboratory, Golden, Colorado 80401, United States*

Joshua T. Koubek − *Department of Chemistry, Colorado School of Mines, Golden, Colorado 80401, United States*

Sarah Zaccarine − *Department of Chemistry, Colorado School of Mines, Golden, Colorado 80401, United States*

Rachel E. Mow − *National Renewable Energy Laboratory, Golden, Colorado 80401, United States; Department of Chemistry, Colorado School of Mines, Golden, Colorado 80401, United States*

Svitlana Pylypenko − *National Renewable Energy Laboratory, Golden, Colorado 80401, United States; Department of Chemistry, Colorado School of Mines, Golden, Colorado 80401, United States;* orcid.org/0000-0001-7982-734X

Alan Sellinger − *National Renewable Energy Laboratory, Golden, Colorado 80401, United States; Department of Chemistry, Colorado School of Mines, Golden, Colorado 80401, United States;* orcid.org/0000-0001-6705-1548

Thomas Gennett − *National Renewable Energy Laboratory, Golden, Colorado 80401, United States; Department of Chemistry, Colorado School of Mines, Golden, Colorado 80401, United States*

Complete contact information is available at: https://pubs.acs.org/10.1021/acsmaterialslett.9b00413

Author Contributions

The manuscript was written through contributions of all authors. All authors have given approval to the final version of the manuscript.

Notes

The views expressed in the article do not necessarily represent the views of the DOE or the U.S. Government. The U.S. Government retains and the publisher, by accepting the article for publication, acknowledges that the U.S. Government retains a nonexclusive, paid-up, irrevocable, worldwide license to publish or reproduce the published form of this work, or allow others to do so, for U.S. Government purposes.

The authors declare no competing financial interest.

■ ACKNOWLEDGMENTS

This work was authored in part by Alliance for Sustainable Energy, LLC, the manager and operator of the National Renewable Energy Laboratory for the U.S. Department of Energy (DOE) under Contract No. DE-AC36-08GO28308. Funding provided by the Hydrogen Materials—Advanced Research Consortium (HyMARC), established as part of the Energy Materials Network under the U.S. Department of Energy, Office of Energy Efficiency and Renewable Energy, Fuel Cell Technologies Office. Use of the Stanford Synchrotron Radiation Lightsource, SLAC National Accelerator Laboratory, is supported by the U.S. Department of Energy, Office of Science, Office of Basic Energy Sciences under Contract No. DE-AC02-76SF00515. Prof. James Ranville and Mr. Logan Rand of Colorado School of Mines are acknowledged for their help in ICP-AES experiments and data analysis of the COFs reported in this study.

■ REFERENCES

(1) Feng, X.; Ding, X.; Jiang, D. Covalent organic frameworks. *Chem. Soc. Rev.* **2012**, *41*, 6010−6022.

(2) Waller, P. J.; Gandara, F.; Yaghi, O. M. Chemistry of Covalent Organic Frameworks. *Acc. Chem. Res.* **2015**, *48*, 3053−3063.

(3) Bisbey, R. P.; Dichtel, W. R. Covalent Organic Frameworks as a Platform for Multidimensional Polymerization. *ACS Cent. Sci.* **2017**, *3*, 533−543.

(4) Hughes, B. K.; Braunecker, W. A.; Bobela, D. C.; Nanayakkara, S. U.; Reid, O. G.; Johnson, J. C. Covalently Bound Nitroxyl Radicals in an Organic Framework. *J. Phys. Chem. Lett.* **2016**, *7*, 3660−3665.

(5) Hu, Y.; Dunlap, N.; Wan, S.; Lu, S.; Huang, S.; Sellinger, I.; Ortiz, M.; Jin, Y.; Lee, S.-h.; Zhang, W. Crystalline Lithium Imidazolate Covalent Organic Frameworks with High Li-Ion Conductivity. *J. Am. Chem. Soc.* **2019**, *141*, 7518−7525.

(6) Ding, X.; Chen, L.; Honsho, Y.; Feng, X.; Saengsawang, O.; Guo, J.; Saeki, A.; Seki, S.; Irle, S.; Nagase, S.; Parasuk, V.; Jiang, D. An n-channel two-dimensional covalent organic framework. *J. Am. Chem. Soc.* **2011**, *133*, 14510−14513.

(7) Guo, J.; Xu, Y.; Jin, S.; Chen, L.; Kaji, T.; Honsho, Y.; Addicoat, M. A.; Kim, J.; Saeki, A.; Ihee, H.; Seki, S.; Irle, S.; Hiramoto, M.; Gao, J.; Jiang, D. Conjugated organic framework with three-dimensionally ordered stable structure and delocalized pi clouds. *Nat. Commun.* **2013**, *4*, 2736.

(8) Ding, S.-Y.; Gao, J.; Wang, Q.; Zhang, Y.; Song, W.-G.; Su, C.-Y.; Wang, W. Construction of Covalent Organic Framework for Catalysis: Pd/COF-LZU1 in Suzuki−Miyaura Coupling Reaction. *J. Am. Chem. Soc.* **2011**, *133*, 19816−19822.

(9) Wu, Y.; Xu, H.; Chen, X.; Gao, J.; Jiang, D. A π-electronic covalent organic framework catalyst: π-walls as catalytic beds for Diels-Alder reactions under ambient conditions. *Chem. Commun.* **2015**, *51*, 10096−10098.

(10) Wang, X.; Han, X.; Zhang, J.; Wu, X.; Liu, Y.; Cui, Y. Homochiral 2D Porous Covalent Organic Frameworks for Heterogeneous Asymmetric Catalysis. *J. Am. Chem. Soc.* **2016**, *138*, 12332−12335.

(11) Huang, N.; Zhai, L.; Xu, H.; Jiang, D. Stable Covalent Organic Frameworks for Exceptional Mercury Removal from Aqueous Solutions. *J. Am. Chem. Soc.* **2017**, *139*, 2428−2434.

(12) Wang, W.; Deng, S.; Ren, L.; Li, D.; Wang, W.; Vakili, M.; Wang, B.; Huang, J.; Wang, Y.; Yu, G. Stable Covalent Organic Frameworks as Efficient Adsorbents for High and Selective Removal of an Aryl-Organophosphorus Flame Retardant from Water. *ACS Appl. Mater. Interfaces* **2018**, *10*, 30265−30272.

(13) Furukawa, H.; Yaghi, O. M. Storage of hydrogen, methane, and carbon dioxide in highly porous covalent organic frameworks for clean energy applications. *J. Am. Chem. Soc.* **2009**, *131*, 8875−8883.

(14) Huang, N.; Chen, X.; Krishna, R.; Jiang, D. Two-dimensional covalent organic frameworks for carbon dioxide capture through channel-wall functionalization. *Angew. Chem., Int. Ed.* **2015**, *54*, 2986−2990.
(15) Huang, N.; Krishna, R.; Jiang, D. Tailor-Made Pore Surface Engineering in Covalent Organic Frameworks: Systematic Functionalization for Performance Screening. *J. Am. Chem. Soc.* **2015**, *137*, 7079−7082.
(16) Suh, M. P.; Park, H. J.; Prasad, T. K.; Lim, D.-W. Hydrogen Storage in Metal-Organic Frameworks. *Chem. Rev.* **2012**, *112*, 782−835.
(17) Turnes Palomino, G.; Llop Carayol, M. R.; Otero Arean, C. Thermodynamics of hydrogen adsorption on the zeolite Ca-Y. *Catal. Today* **2008**, *138*, 249−252.
(18) Kapelewski, M. T.; Geier, S. J.; Hudson, M. R.; Stuck, D.; Mason, J. A.; Nelson, J. N.; Xiao, D. J.; Hulvey, Z.; Gilmour, E.; FitzGerald, S. A.; Head-Gordon, M.; Brown, C. M.; Long, J. R. M2(m-dobdc) (M = Mg, Mn, Fe, Co, Ni) metal-organic frameworks exhibiting increased charge density and enhanced H_2 binding at open metal sites. *J. Am. Chem. Soc.* **2014**, *136*, 12119−12129.
(19) Allendorf, M. D.; Hulvey, Z.; Gennett, T.; Ahmed, A.; Autrey, T.; Camp, J.; Seon Cho, E.; Furukawa, H.; Haranczyk, M.; Head-Gordon, M.; Jeong, S.; Karkamkar, A.; Liu, D.-J.; Long, J. R.; Meihaus, K. R.; Nayyar, I. H.; Nazarov, R.; Siegel, D. J.; Stavila, V.; Urban, J. J.; Veccham, S. P.; Wood, B. C. An assessment of strategies for the development of solid-state adsorbents for vehicular hydrogen storage. *Energy Environ. Sci.* **2018**, *11*, 2784−2812.
(20) Mendoza-Cortes, J. L.; Goddard, W. A.; Furukawa, H.; Yaghi, O. M. A Covalent Organic Framework that Exceeds the DOE 2015 Volumetric Target for H_2 Uptake at 298 K. *J. Phys. Chem. Lett.* **2012**, *3*, 2671−2675.
(21) Dodson, R. A.; Wong-Foy, A. G.; Matzger, A. J. The Metal-Organic Framework Collapse Continuum: Insights from Two-Dimensional Powder X-ray Diffraction. *Chem. Mater.* **2018**, *30*, 6559−6565.
(22) Denysenko, D.; Grzywa, M.; Jelic, J.; Reuter, K.; Volkmer, D. Scorpionate-Type Coordination in MFU-4l Metal-Organic Frameworks: Small-Molecule Binding and Activation upon the Thermally Activated Formation of Open Metal Sites. *Angew. Chem., Int. Ed.* **2014**, *53*, 5832−5836.
(23) Duarte, T. A. G.; Carvalho, A. P.; Martins, L. M. D. R. S. Ultrafast and selective oxidation of styrene to benzaldehyde catalyzed by a C-scorpionate Cu(II) complex. *Catal. Sci. Technol.* **2018**, *8*, 2285−2288.
(24) Braunecker, W. A.; Hurst, K. E.; Ray, K. G.; Owczarczyk, Z. R.; Martinez, M. B.; Leick, N.; Keuhlen, A.; Sellinger, A.; Johnson, J. C. Phenyl/perfluorophenyl stacking interactions enhance structural order in 2D covalent organic frameworks. *Cryst. Growth Des.* **2018**, *18*, 4160−4166.
(25) Chen, X.; Huang, N.; Gao, J.; Xu, H.; Xu, F.; Jiang, D. Towards covalent organic frameworks with predesignable and aligned open docking sites. *Chem. Commun.* **2014**, *50*, 6161−6163.
(26) Chen, X.; Addicoat, M.; Jin, E.; Zhai, L.; Xu, H.; Huang, N.; Guo, Z.; Liu, L.; Irle, S.; Jiang, D. Locking covalent organic frameworks with hydrogen bonds: general and remarkable effects on crystalline structure, physical properties, and photochemical activity. *J. Am. Chem. Soc.* **2015**, *137*, 3241−3247.
(27) Kandambeth, S.; Venkatesh, V.; Shinde, D. B.; Kumari, S.; Halder, A.; Verma, S.; Banerjee, R. Self-templated chemically stable hollow spherical covalent organic framework. *Nat. Commun.* **2015**, *6*, 6786.
(28) Mu, M.; Wang, Y.; Qin, Y.; Yan, X.; Li, Y.; Chen, L. Two-Dimensional Imine-Linked Covalent Organic Frameworks as a Platform for Selective Oxidation of Olefins. *ACS Appl. Mater. Interfaces* **2017**, *9*, 22856−22863.
(29) Jiang, D.; Chen, X.; Geng, K.; Liu, R.; Tan, K. T.; Gong, Y.; Li, Z.; Tao, S.; Jiang, Q. Covalent Organic Frameworks: Chemical Approaches to Designer Structures and Built-in Functions. *Angew. Chem., Int. Ed.* **2019**, DOI: 10.1002/anie.201904291.
(30) Vigato, P. A.; Tamburini, S. The challenge of cyclic and acyclic Schiff bases and related derivatives. *Coord. Chem. Rev.* **2004**, *248*, 1717−2128.
(31) Gupta, K. C.; Sutar, A. K. Catalytic activities of Schiff base transition metal complexes. *Coord. Chem. Rev.* **2008**, *252*, 1420−1450.
(32) Cano, E.; Bastidas, J. M. Effect of Relative Humidity on Copper Corrosion by Acetic Acid and Formic Acid Vapours. *Can. Metall. Q.* **2002**, *41*, 327−336.
(33) Zhang, G.; Yi, H.; Zhang, G.; Deng, Y.; Bai, R.; Zhang, H.; Miller, J. T.; Kropf, A. J.; Bunel, E. E.; Lei, A. Direct Observation of Reduction of Cu(II) to Cu(I) by Terminal Alkynes. *J. Am. Chem. Soc.* **2014**, *136*, 924−926.
(34) Kau, L. S.; Spira-Solomon, D. J.; Penner-Hahn, J. E.; Hodgson, K. O.; Solomon, E. I. X-ray absorption edge determination of the oxidation state and coordination number of copper. Application to the type 3 site in Rhus vernicifera laccase and its reaction with oxygen. *J. Am. Chem. Soc.* **1987**, *109*, 6433−6442.
(35) Lamberti, C.; Bordiga, S.; Bonino, F.; Prestipino, C.; Berlier, G.; Capello, L.; D'Acapito, F.; Llabres i Xamena, F. X.; Zecchina, A. Determination of the oxidation and coordination state of copper on different Cu-based catalysts by XANES spectroscopy in situ or in operando conditions. *Phys. Chem. Chem. Phys.* **2003**, *5*, 4502−4509.
(36) Prestipino, C.; Regli, L.; Vitillo, J. G.; Bonino, F.; Damin, A.; Lamberti, C.; Zecchina, A.; Solari, P. L.; Kongshaug, K. O.; Bordiga, S. Local Structure of Framework Cu(II) in HKUST-1 Metallorganic Framework: Spectroscopic Characterization upon Activation and Interaction with Adsorbates. *Chem. Mater.* **2006**, *18*, 1337−1346.
(37) Neylon, M. K.; Marshall, C. L.; Kropf, A. J. In Situ EXAFS Analysis of the Temperature-Programmed Reduction of Cu-ZSM-5. *J. Am. Chem. Soc.* **2002**, *124*, 5457−5465.
(38) Farjas, J.; Roura, P. Exact analytical solution for the Kissinger equation: Determination of the peak temperature and general properties of thermally activated transformations. *Thermochim. Acta* **2014**, *598*, 51−58.
(39) Kazansky, V. B.; Pidko, E. A. A new insight in the unusual adsorption properties of Cu+ cations in Cu-ZSM-5 zeolite. *Catal. Today* **2005**, *110*, 281−293.
(40) Kubas, G. J. Fundamentals of H2 Binding and Reactivity on Transition Metals Underlying Hydrogenase Function and H2 Production and Storage. *Chem. Rev.* **2007**, *107*, 4152−4205.
(41) Panella, B.; Hirscher, M.; Roth, S. Hydrogen adsorption in different carbon nanostructures. *Carbon* **2005**, *43*, 2209−2214.
(42) Goldsmith, J.; Wong-Foy, A. G.; Cafarella, M. J.; Siegel, D. J. Theoretical Limits of Hydrogen Storage in Metal-Organic Frameworks: Opportunities and Trade-Offs. *Chem. Mater.* **2013**, *25*, 3373−3382.

https://dx.doi.org/10.1021/acsmaterialslett.9b00413
ACS Materials Lett. 2020, 2, 227−232